

---

# Planning with Generative Cognitive Maps

---

**Jeffrey Qin\*, Albert Yang\* & Cole Wyeth**  
Computer Science  
University of Waterloo  
{jzqin, aj5yang, cwyeth}@uwaterloo.ca

**Ziheng Xu**  
Dyson School of Applied Economics & Mgmt  
Cornell University  
zx342@cornell.edu

**Kevin Ellis**  
Department of Computer Science,  
Cornell University  
kellis@cornell.edu

**Marta Kryven**  
Computer Science, Dalhousie University  
and Brain and Cognitive Sciences, MIT  
marta.kryven@dal.ca

## Abstract

Planning relies on cognitive maps – models that encode world structure given cognitive resource constraints. The problem of learning functional cognitive maps is shared by humans, animals and machines. However, we still lack a clear understanding of how people represent maps for planning, particularly when the goal is to support cost-efficient plans. We take inspiration from theory of compositional mental representations in cognitive science to propose GenPlan: a cognitively-grounded computational framework that models redundant structure in maps and saves planning cost through policy reuse. Our framework integrates (1) a Generative Map Module that infers generative compositional structure and (2) a Structure-Based Planner that exploits structural redundancies to reduce planning costs. We show that our framework closely aligns with human behavior, suggesting that people approximate planning by piecewise policies conditioned on world structure. We also show that our approach reduces the computational cost of planning while producing good-enough plans, and contribute a proof-of-concept implementation demonstrating how to build these principles into a working system.

## 1 Introduction

People are highly proficient in solving real-world planning problems. For example, we can navigate cities without precisely knowing every link in the street network (Fig. 1a.)[Bongiorno et al., 2021] and accomplish complex construction projects (Fig. 1b.) with many actions and sub-goals [Mugan et al., 2024]. Solving these problems optimally is theoretically intractable [Kaelbling et al., 1998], and therefore approximate algorithms for planning in natural domains remain an active area of research in AI [Silver and Veness, 2010], robotics [Curtis et al., 2025], and cognitive science [Kryven et al., 2024, van Opheusden et al., 2023]. Here, we seek to uncover cognitive computations that enable humans to plan efficiently in natural domains. To do this, we focus on the key intuition that the human world is structured (Fig.1c,d) and propose that people reason about redundancies in this structure to efficiently encode cognitive maps, and reduce planning costs. We formalize this hypothesis in GenPlan, a computational model that gives an algorithmic account of how structure-based planning can be implemented in practice.

Formally, a planning problem constitutes a search within a decision tree that describes possible states and actions [Kuperwajs et al., 2025, Russell and Norvig, 2016]. This tree can be encoded

---

\*Equal contribution.

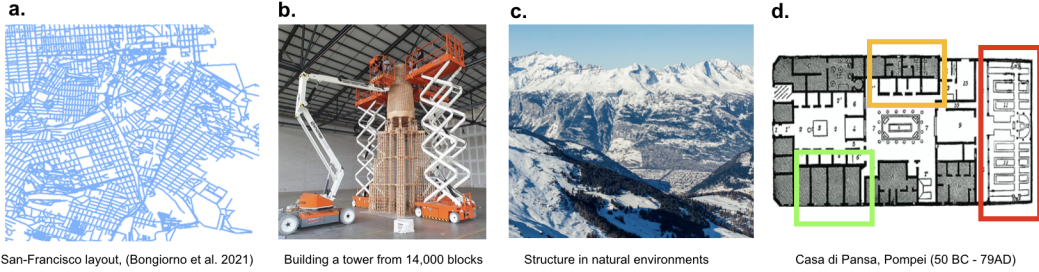


Figure 1: Structured human environments: city street networks, construction projects, natural landscapes, and an interior floor-plan with repeating structural elements highlighted. People learn mental world-models that exploit this structure to make resource-efficient plans.

as a learned neural policy [Liu et al., 2020], an explicit tree structure [Russell and Norvig, 2016, Silver and Veness, 2010], or a model describing states and actions in a symbolic form [Tang et al., 2024]. The size of the underlying state-space determines the computational cost of the problem, or how difficult it should be. Since optimal planning beyond non-trivial state-spaces is intractable, approximate planning frameworks have focused on building partial state-spaces [Silver and Veness, 2010], learning generalizable policies [Curtis et al., 2022, Singh et al., 2012], and grouping actions frequently performed together into options [Sutton et al., 1999]. However, the difficulty predicted by these approximate planning algorithms rarely aligns with human experience, as people often solve formally complex real-world problems with relative ease.

We take inspiration from the theory of *compositional concepts* in cognitive science, which states that humans learn complex concepts by combining simpler ones [Fodor, 1975, Lake and Piantadosi, 2020, Pitt et al., 2021], and adapt the principle of compositionality to model human cognitive maps and plans as generative structures. Compositionality has been successful in explaining concept representation in visual [Lake and Piantadosi, 2020, Tian et al., 2020], auditory [Verhoef et al., 2014, Rohrmeier, 2020, Hofer et al., 2021] and spatial domains [Sharma et al., 2022, McCarthy et al., 2021]. Further, compositional reasoning is culturally universal [Pitt et al., 2021], suggesting that it may be an evolved adaptation to natural structure people encounter in daily life [Johnston et al., 2022]. Neural and behavioral studies provide ample evidence that cognitive maps are represented using similar compositional generative structures. Neural evidence from human studies includes mirror-invariant encoding of natural scenes [Dilks et al., 2011] and reuse of neural reference frames across similar environments [Marchette et al., 2014]. Behavioral evidence includes hierarchical spatial representations [Kosslyn et al., 1974, Stevens and Coupe, 1978, Hirtle and Jonides, 1985] reflected in first planning routes between, and then within semantic regions [Bailenson et al., 2000, Newcombe et al., 1999, Wiener and Mallot, 2003, Wang and Brockmole, 2003, Balaguer et al., 2016, Tomov et al., 2020], and ability to predict unseen environment layout in structured environments [Sharma et al., 2022].

In formal terms, combinatorial concept representations can be modeled by *mental programs* – symbolic instructions specifying how to produce new instances of a given concept class [Lake et al., 2015, Lake and Piantadosi, 2020]. Computational accounts of concept learning as *program induction* (inferring a program from a given a set of examples) provide powerful explanations of human learning efficiency – only a few examples can suffice to deduce an underlying program, in contrast to vast amounts of data required by purely neural models [Tenenbaum et al., 2011, Lake et al., 2015]. Building on this research, we model cognitive maps as generative programs that capture structures such as symmetries and repeated parts, and propose an algorithmic framework that models cost-efficient planning in such maps by reusing local policy conditioned on structure, instead of solving a global optimization problem.

In this work we adopt a scientific and an engineering goal: (1) to understand computational cognitive principles by which humans plan in structured spatial domains, and (2) to engineer a cost-efficient computational framework that formalizes human-like planning in structured environments. We contribute:

- Generative Map Module (GMM), which discovers programmatic map representations using tractable inference;

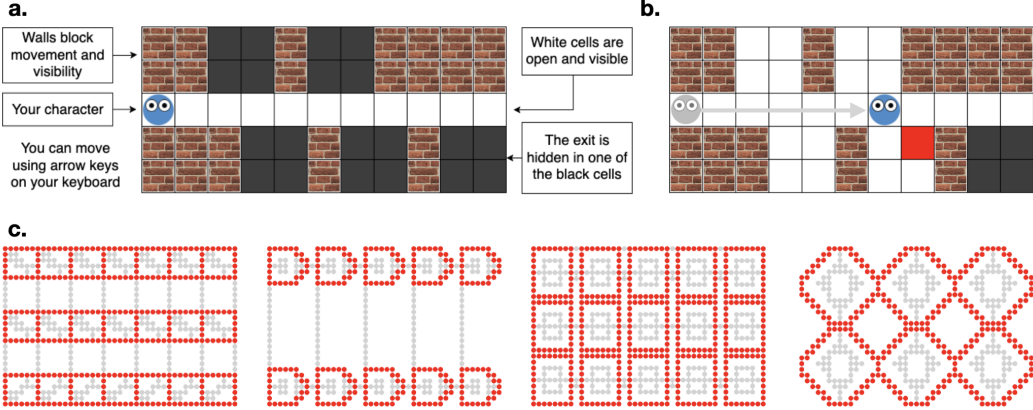


Figure 2: The Maze Search Task with structured layouts. (a.) Task Setup illustrated in a simple example. Participants can use keyboard keys to navigate over any non-wall cells. The exit is initially hidden in one of the black (unobserved) cells. (b.) The exit is shown as a red tile when it comes into view. (c.) A subset of structures environment layouts used to evaluate GenPlan and compare its performance to that of a Naive POMCP. The dots denote floor cells through which participants can move. Red dots denote structural unit boundaries.

- Structure-Based Planner (SBP) that implements hierarchical planning both within and between the structural units
- Empirical validation of our framework on human behavior, showing that human planning is consistent with generative cognitive maps and policy reuse.

The GMM models observations of the environment by inferring a small distribution over programmatic maps. To do this, we use a Large Language Model (LLM) as an embedding of human priors learned through training on human data. The SBP extends a Partially Observable Markov Decision Process (POMDP) to use the GMM representation. It constructs end-to-end policies for within-unit planning and between-unit transitions using adaptations of a Partially Observable Monte Carlo Planner (POMCP). In the next section, we introduce the experimental environment, followed by a detailed description of computational models. In Section 3, we compare our models’ predictions with human empirical results.

## 2 Methods

### 2.1 Structured Spatial Domain

We examine people’s planning strategies by adapting a version of Maze Search Task (MST) previously used to study human behavior in spatial navigation domains [Kryven et al., 2024, 2021, Geva-Sagiv et al., 2025]. The objective of MST is to navigate a series of partially observable, two-dimensional grid-worlds, finding exits hidden in each. Each environment has only one exit. The environments are partially observable, with the exits initially placed at a random unobserved location (black cells). Fig.2 shows a simple MST environment seen by participants during one of the practice trials<sup>3</sup>. People navigate by using their keyboard keys to move to any unoccupied grid cells adjacent to their character (a round avatar). The black hidden cells are revealed when they come into the avatar’s line of sight. When revealed, the exit becomes visible as a red tile. As soon as the character moves over the exit, the trial ends. In our adaptation of MST all mazes are structured, and contained between 2 and 20 repeating structural units. The units may have occurred as reflected or rotated instances, where the structured area comprised between 80 - 100% of the environment layout.

<sup>3</sup>A demo is available here: [http://18.25.132.241/fragments/int\\_exp.php](http://18.25.132.241/fragments/int_exp.php)

## 2.2 Computational Models

Decision making under partial observability can be modeled by a partially observable Markov decision process (POMDP). Equivalently, it can be viewed as a fully observable search through a space of beliefs, where each belief is a probability distribution over possible states. Solving POMDPs is notoriously hard [Madani et al., 2003], hence understanding how people approach these problems holds deep importance for cognitive science and AI.

Formally, a POMDP is a tuple  $\langle \Delta(S), A, \tau, r, b_0, \gamma \rangle$ , where  $\Delta(S)$  is the space of probability distributions over a state space  $S$ ,  $A$  is the set of actions,  $\tau$  is the belief update function,  $r$  is the reward function,  $b_0$  is the initial belief, and  $\gamma$  is the discount factor. The belief state evolves deterministically via  $\tau$ , reflecting both the agent's actions and observations.

In this work, each state  $s \in S$  is represented as an  $N \times M$  grid whose cells are labeled {wall, empty, exit, agent}. The overall state space  $S$  consists of all such grids containing exactly one agent and one exit. A belief  $b \in \Delta(S)$  is thus a probability distribution over these grids, encoding the agent's uncertainty about the true state. Initially,  $b_0$  assumes that the agent and the walls are known, while the exit is uniformly distributed over all valid, unseen cells. The action space  $A$  contains four possible movements (up, down, left, right). Observations  $o \in O$  reveal the visible subset of the grid around the agent, with each visible cell labeled {wall, empty, exit}, and any cell outside the agent's visibility range  $r$  labeled as *unseen*. Observations are consistent with the grid structure of the true state  $s \in S$ .

The belief update function  $\tau$  is given by

$$b'(s') \propto Z(o | s') \sum_{s \in S} T(s', a, s) b(s),$$

where  $T(s', a, s)$  is the transition function, and  $Z(o | s')$  is the observation likelihood. The transition function  $T(s', a, s)$  specifies the probability of transitioning to state  $s'$  from  $s$  after executing action  $a$ . Here, actions that would move the agent into a wall result in the agent remaining in its current position, and transitions to an exit state terminate the process. The observation function  $Z(o | s')$  encodes the likelihood of observing  $o$  given  $s'$ , where observations reflect the visible subset of the grid within range  $r$  of the agent's position. Visibility is blocked by walls, such that cells beyond a wall are labeled as *unseen*. Finally, the reward function  $r(b, a)$  is the expected reward under the belief  $b$ . Since the agent can always see an exit before reaching it,  $r(b, a) = 1$  if action  $a$  leads the agent to a known exit and 0 otherwise.

**Expected Utility** The optimal policy for this POMDP can be found through a belief space tree search [Kaelbling et al., 1998]. The search is conducted over a tree where each node represents a belief  $b \in \Delta(S)$ , and edges correspond to action-observation pairs  $(a, o)$ . Starting from the root node  $b_0$ , the tree expands by simulating actions  $a \in A$  and updating beliefs using the belief update function  $\tau$ . For each action  $a$ , the agent considers all possible observations  $o \in O$ , with the likelihood of each observation determined by the observation function  $Z(o | s')$ . At each node, the value of a belief is computed recursively using the Bellman equation:

$$V(b) = \max_{a \in A} \left[ r(b, a) + \gamma \sum_{o \in O} P(o | b, a) V(\tau(b, a, o)) \right], \quad (1)$$

where  $P(o | b, a)$  is the probability of receiving observation  $o$  after taking action  $a$  under belief  $b$ . The optimal policy  $\pi^*$  is derived by selecting the action at each belief node that maximizes the expected value. See [Kryven et al., 2024] for further details on this implementation, which was used as a model of human planning in MST in prior work.

Although this is the optimal strategy, human behavior has previously been shown to diverge at times from its predictions [Kryven et al., 2024], where the extent of this divergence varies between individuals in a way that can be explained by the amount of cognitive resources people allocate to planning [Kryven et al., 2021]. Previous work with MST, as well as with related non-spatial planning tasks [Huys et al., 2015], has found that people's divergence from the optimal trajectories is most readily explained by a limited planning horizon (discount factor  $\gamma < 1$  in Equation 1). In the remainder of this section we describe alternative computational hypotheses for how humans could make decisions in this environment by reasoning about structural patterns.

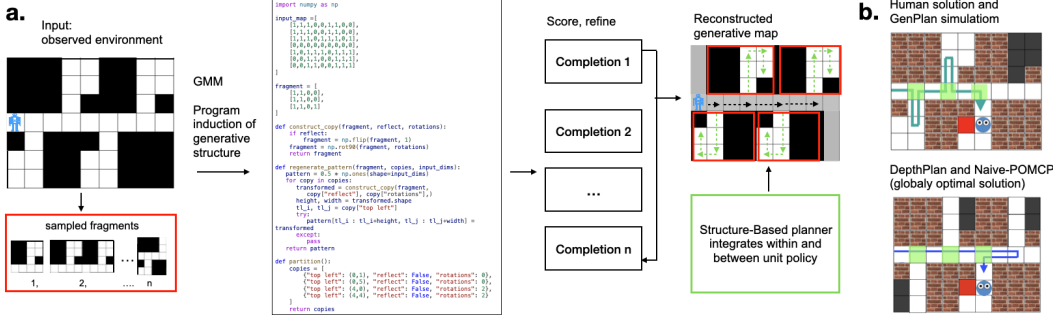


Figure 3: Model Architecture and predictions. (a) The GenPlan Framework. GMM recovers a small distribution over generative maps based on input (a partial observation of the ground truth map). Each generative map constitutes a set of candidate units coupled with a program for reconstructing the input from them. We assign a likelihood to each generative map, and pass the most likely reconstruction to SBP. SBP plans a policy once for each structural unit. (b) A human solution to the given example agrees with prediction of GenPlan (top panel). Arrows indicate the participant’s path. The path predicted by alternative models DepthPlan and Naive-POMCP (bottom panel) instead optimizes the global policy. Green highlighting shows discriminating decisions.

**Generative Structure-Based Framework (GenPlan)** Next, we describe a modeling framework that formalizes planning strategies conditioned on automatically discovered latent structure of the state-space. Our model consists of two modules: a Generative Map Module (GMM) and Structure-Based Planner (SBP). See Fig.3 for a high-level overview of this architecture. The GMM recovers a programmatic representation of the observed state-space as a composition of structural units. The SBP then uses a planner to plan a piece-wise policy once per-unit, in contrast to a global policy, saving computing costs. Importantly, this reconstructed programmatic representation is a cognitively-inspired state-space compression. While such a reconstruction may match the ground-truth planning state-space, it does not need to be exact as long as it is sufficient to serve the agent’s goals [Ho et al., 2022]. In theory, the cognitive principle of combining automatic structure discovery with structure-aware planners can apply to any domain, as a proof of concept here we focus on spatial tasks.

**Generative Map Module (GMM)** Let  $I$  be the global partially observed input grid map of cells  $S_I$ . Here, we assume that  $I$  specifies all wall locations, however, in the general case, it can be any initial partial observation.

The GMM implements approximate inference of a posterior distribution  $p(\mathcal{M}|I)$  over cognitive maps  $\mathcal{M}$  that partition  $I$  into structural units  $\mathcal{M} = \{U_i\}_{i=1}^m$ . We use LLM-based program synthesis with GPT4 to search for programs that generate  $\mathcal{M}$  based on  $I$  (Fig. 3). To do this, we prompt LLM to identify redundant units in the input map, and synthesize a Python program that approximately reconstructs the input from them. The prompt includes Python code with functions describing admissible transformations, as well as a likelihood function for a given  $\mathcal{M}$ . In our implementation the input map  $I$  is a grid-world, specified by an numerical array, where each grid cell is associated with a number (e.g. wall=1, floor=0). The reconstructions  $\mathcal{M}$  do not allow overlapping units, and allow any units that repeat in  $I$  at least twice.

To develop a space of possible map representations, we estimate the likelihood of each candidate  $\mathcal{M}$  by a weighted combination of grid-level similarity, a function of total information in a candidate unit, and the Minimum Description Length (MDL) principle [Rissanen, 1978]. MDL penalizes each unit occurrence by the bits necessary to specify the map reconstruction: their locations (effectively, the number of copies), rotations and reflections. This means that reconstructions made up of many smaller pieces are less likely than reconstructions made up of bigger ones. The function of total information in a unit ensures that the selected units are neither trivial (e.g., uniform blocks of cells made up of either walls or open space) nor noise, by defining an inverted-U relationship between likelihood and informativeness [Kidd et al., 2012]. This treats large units where perception is subject to information bottleneck constraints as less likely [Cheyette and Piantadosi, 2020]. Overall, this likelihood function can express a weighted preference for (1) more accurate reconstructions, (2) simple generative programs (where the programs use primitives transformations and symmetries

relevant to planning), and (3) simpler units. To form the posterior  $p(\mathcal{M}|I)$ , we use the likelihood:

$$l(\mathcal{M}; I) \propto \frac{w_1}{d_x \cdot d_y} \sum_{x=1}^{d_x} \sum_{y=1}^{d_y} (I(x, y) - O(x, y))^2 - w_2 |\mathcal{M}| + w_3 \exp\left(-\frac{(H_{\text{total}} - \beta)^2}{2\sigma^2}\right), \quad (2)$$

where  $d_x, d_y$  are input dimensions,  $O$  is the output (reconstructed map), and  $w_i$  are weights associated with reconstruction accuracy, map complexity, and unit complexity – free parameters of the model. We define the total entropy in the unit as  $H_{\text{total}} = d_x d_y \cdot (-p \log_2 p - (1-p) \log_2(1-p))$ , where  $p$  is the fraction of 1’s in the array, and free parameter  $\beta$  reflects the processing bottleneck, in line with perceptual models explored in prior work [Cheyette and Piantadosi, 2020, Kryven et al., 2024]. This definition ensures that the information term next to  $w_3$  reaches a maximum of 1 when  $H_{\text{total}} = \beta$ , but decays to 0 on both sides of this maximum. In the general case, input  $I$  and output  $O$  are real-valued 2D image arrays. In our current implementation input  $I$  takes values 0 and 1, and the output  $0 \leq O(x, y) \leq 1$ . Instead of using the raw Python program for  $\lambda$  to measure its complexity, we use a compressed encoding of the units and their transformations used to reconstruct the map. Here, compressing LLM-generated output and transformations is analogous to refactoring the synthesized programs. As the length of LLM-synthesized code may be noisy, due to injected comments and code redundancies, refactoring the output obtains a denoised metric of complexity.

The posterior  $p(\mathcal{M}|I)$  defines how the environment structure is encoded into memory. The free parameters  $w_i, \beta$  balance reconstruction accuracy against the complexity of the generative structure and planning costs. In the general case, the framework can maintain a distribution over generative maps, and switch between them at execution time to resolve local observations. In our proof-of-concept implementation we make a simplifying assumption to use the most likely generative map in the SBP module for generating a policy. Fig.3 shows a simple example with structural units highlighted in red. Bigger examples designed in our simulation experiment are shown in Fig.2.

**Structure-Based Planner (SBP)** Implementing SBP integrates planning within and between structural units. Since finding an exact solution is intractable due to the size of the problem [Kaelbling et al., 1998], we solve planning *within a unit* by searching through the belief space using an approximate online Partially Observable Monte Carlo Planner (POMCP) [Silver and Veness, 2010]. A plan *in-between units* consists of leaving the current unit and transitioning to the next one. We solve the former by adapting Monte Carlo Tree Search (MCTS), and introducing an optimistic heuristic valuation for open cells around the boundary of a unit (i.e. cells through which we can exit the unit). Upon completing a plan for the current unit, this heuristic should encourage us to leave the unit in the direction that minimizes the expected global cost of reaching the exit. In the general case, this can be any heuristic that does not overestimate the true cost. Here, we compute the values of boundary cells as inversely proportional to the average of manhattan distances to the remaining external unobserved cells, hence assigning a higher value to cells that are on average closer to the remaining unseen parts of the map. We solve the transition to the next unit using a POMCP on the global map, but implement the option to switch to within-unit planning upon reaching the new unit. Here, we evaluate the option by estimating the average per-step cost to plan within the unit. This value scales with the complexity of the unit, and is optimal when a reusable policy can be applied.

### 2.3 Computational Hypotheses

We compare human performance to the hypotheses (planing algorithms) to evaluate whether and how human planning implements the two computational steps outlined by GenPlan.

1. **Structure-Naive Planner (Naive-POMCP):** The model doesn’t use generative maps, and plans by optimizing a global policy for the environment.
2. **Structure-Naive Planner With Cognitive Constraints (DepthPlan)** The model doesn’t use generative maps, and plans by optimizing a global policy that discounts future states to model limited planning depth. This model was previously used to describe how people plan in MST [Kryven et al., 2024].
3. **A Generative Planner (Gen-POMCP):** The model uses generative maps, and plans a reusable policy based on the most likely map from the distribution of induced maps  $p(\mathcal{M}|I)$  (see Fig. 3a and b).

Naive-POMCP uses an approximate POMCP planner designed for large partially-observable state-spaces. It was previously used to model human planning in large domains, although this work did not examine the effect of environment structure on human plans [Sharma et al., 2022]. DepthPlan is consistent with prior work that models human deviations from optimal cost minimization by limited planning horizon, without modeling environment structure [Kryven et al., 2024, Huys et al., 2015]. Since DepthPlan internally computes an optimal policy, it can only be applied to smaller environments (generally 6 or fewer structural units, see Experiment 1). Only the third hypothesis is consistent with the two computational steps proposed by the GenPlan framework: it represents maps as generative programs, and uses this structure to plan a reusable policy, reducing planning costs.

### 3 Experiments

We first test whether people use structure to reduce computational costs of planning, as implemented by Gen-POMCP, in contrast to DepthPlan – the state-of-the-art model of planning in MST Kryven et al. [2024] (Experiment 1). For this experiment, we use a set of 20 structured environments at a scale that can be solved by DepthPlan, in order to compare DepthPlan and Gen-POMCP. A preliminary pilot study revealed a strong effect of structure on planning, leading us to conclude that a sample of  $N=30$  participants is sufficient to confirm this effect. We then run a simulation experiment with 10 large environments containing 20-25 units (Experiment 2) to compare the computational costs of Gen-POMCP and Naive-POMCP, demonstrating that Gen-POMCP requires significantly fewer computational resources.

#### 3.1 Experiment 1: Behavioral Validation

**Procedure** The experiment was conducted in a web browser, using the web-interface of MST [Kryven et al., 2024]. Before beginning the experiment participant gave informed consent and completed a series of practice trials, followed by an instruction quiz. Following this, they completed a variant of MST with structured mazes, with exit locations randomly chosen at the time of design. After completing the experiment, we administered a post-experiment questionnaire collecting demographic information. As our goal was to observe ecologically-valid planning, we did not offer performance-based incentives, and simply informed participants that the exit could be in any of the hidden tiles, and instructed them to find it in each environment.

We recruited 30 (13 female, 17 male,  $M(\text{age}) = 36.7$ ,  $SD(\text{age}) = 13.5$ ) english-speaking participants on Prolific, who were paid 9£ per hour. None were excluded. On average the experiment took 10 minutes to complete. The experiment was approved by our institution’s IRB.

**Behavioral metrics** We introduce the following *behavioral definitions* to quantify people’s alignment with the GenPlan framework.

- A set of *discriminating decisions*  $\mathcal{D}(I)$  in a given environment  $I$  is the subset of all states in  $I$  where Gen-POMCP and Depth Plan predict a different most likely action. That is,  $\mathcal{D}(I)$  includes only actions diagnostic of structure-based planning. Fig. 3b illustrates discriminating decisions in a simple example. Unlike the global solution (bottom panel), Gen-POMCP and most humans search by entering inside the structural units. The cells highlighted in green are discriminating decisions.
- *Modular fraction*  $\sigma(\mathcal{D})$  defines the fraction of decisions in a given set of discriminating decisions  $\mathcal{D}$  that are more likely under Gen-POMCP, compared to DepthPlan. Notably, as weights  $w_i$  in equation 2 can tradeoff accuracy against representation and planning costs, Gen-POMCP can capture flexible strategies that integrate global and local search. For simplicity, here we assume stable population-level weights that strongly favor structure over accuracy, meaning that  $\sigma(\mathcal{D})$  is a conservative estimate of how well Gen-POMCP explain human behavior.

**Results** Our results reveal that Gen-POMCP predicts human behavior significantly better than DepthPlan (Fig. 4). Examination of modular fractions for individuals and environments shows that people are highly consistent with our model, demonstrating structure-based planning across all environments and individuals. Across all environments, human behavior is better explained by Gen-POMCP, suggesting that people approximate planning by piecewise policies conditioned on

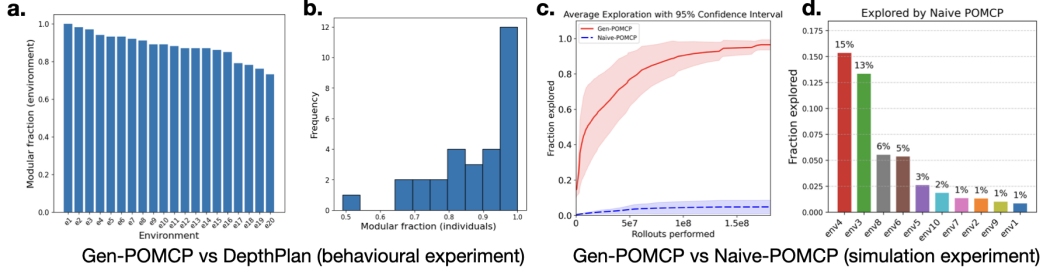


Figure 4: Experiment result shows that Gen-POMCP explains people better than DepthPlan. (a.) Modular fraction for each environment (b.) The histogram of individual modular fractions per participant, over all discriminating decisions. (c) The fraction of each environment explored by Gen-POMCP across environments (solid line) and Naive-POMCP (dashed lines) as a function of compute budget (number of MCTS rollouts). (d) The fraction of each environment explored by Naive-POMCP, if given the amount of MCTS rollouts at which Gen-POMCP fully explores the given environment. Each bar shows a different environment.

structure, rather than by planning a global policy with a limited depth. Fig. 3b illustrates the difference between the models in a simple example. Like Gen-POMCP, the majority of people search the environment by a trajectory shown in the top panel. However, both the optimal policy predicted by the Naive-POMCP, and the depth-limited planning as implemented by DepthPlan, predict the trajectory shown at the bottom – because it allows to quickly reveal a large portion of the global map.

### 3.2 Experiment 2: Simulation

Next, we compare the computing resources needed by Gen-POMCP and Naive-POMCP to explore 10 large structured environments (e.g., see Fig. 2c). As the objective of MST is to find a hidden exit, each simulation is set up to run until the environment is fully explored (i.e., the exit is not revealed until the end of the simulation). We compare two quantitative comparisons. For each environment we compute the fraction of the environment that each model is able to explore given a certain compute budget (Fig. 4d), finding that the Gen-POMCP required a much smaller budget to search the entire environment. Fig. 4c separately shows the fraction of each environment that Naive-POMCP is able to explore, if given the rollout budget at which Gen-POMCP has searched the entire environment. In Appendix B we give a proof that the length of the search trajectories produced by Gen-POMCP exceeds trajectories produced by Naive-POMCP by a bounded amount, demonstrating that Gen-POMCP also produces good enough plans. All environments used in Experiments 1 and 2 are shown in Appendix C.

## 4 Related Work

**Models of Human Planning** People make near-optimal plans in natural domains, such as city navigation [Bongiorno et al., 2021], yet often perform sub-optimally in laboratory-based behavioral paradigms such as multi-arm bandits [Keramati et al., 2016, Huys et al., 2015], strategic games [Ferreira, 2013], and sequential decision-making [Unterrainer et al., 2004, Kryven et al., 2024, Callaway et al., 2022]. Such deviations from optimality are often explained by approximate planning with a limited planning horizon [Ferreira, 2013, Kryven et al., 2024, van Opheusden et al., 2023]. Recent work [Correa et al., 2025] examines how people represent policies in programmatic forms that minimize description lengths, finding sensitivity to both effort minimization (similar to seeking shorter search paths) and MDL (shorter programs). Similar to our work, their study found that human plans heavily favor reuse. Unlike our work, experimental paradigms used in these studies lack the regular problem-domain structure ubiquitous in the real-world.

**Cognitive Maps** A recent study found that people form cognitive maps that facilitate planning [Ho et al., 2022], by selectively representing only the goal-relevant parts of the map. Like our work, this study assumes that human cognitive maps are learned by compressing observations. Unlike our

work, this study uses unstructured maps. A recent study of exploration in structured environments found that people anticipate environment structure, even when not informed about them in advance [Sharma et al., 2022], and can predict unseen parts of the map. Unlike our work, this study focuses solely on map prediction, and does not examine the role of cognitive maps in planning. It also relies on exhaustive enumerative search to discover the underlying map representations, unlike our work that implements tractable inference using LLM-based program synthesis.

**Learning Compressed Policies to Plan.** Reinforcement Learning (RL) models express actions performed together as *options* [Sutton et al., 1999], learn families of similar Markov Decision Process (MDP) with shared rewards [Wilson et al., 2012], and build efficient state-spaces by recognizing actions that lead to identical observations [Singh et al., 2012]. Generalized planning frameworks can find algorithm-like policies for solving multiple instances of a task [Curtis et al., 2022], although studies have not yet considered their alignment with human behavior. A principle of grouping game-board states based on rotation and reflection symmetries was used to optimize representations in the game of Go [Silver et al., 2017]. Unlike our work, these works do not directly consider policy reuse by conditioning on approximate structured state-space representations.

**Natural priors.** Adaptive real-world planning draws on complex prior knowledge of the world [Acquaviva et al., 2022, Spelke and Kinzler, 2007, Dehaene et al., 2006]. Learning natural priors that make people so efficient in real-world remains an important problem in cognitive AI [Kumar et al., 2022, Li et al., 2024, Binz et al., 2024]. [Feldman, 2013]. Similar to our work, an emerging line of research leverages LLMs as a back-end to planning frameworks as a way of informing planning by the implicit natural priors embedded in LLM though training on vast amounts of human data [Tang et al., 2024, Correa et al., 2025, Towers et al., 2024, Xie et al., 2023, Piriayakulkij et al., 2025, Curtis et al., 2025]. Our computational framework builds on this approach, focusing on modeling how cognitive maps and planning policies may be learned together.

## 5 Discussion

We propose a computational framework that (1) represents maps by approximate generative programs and (2) plans in these representations through policy reuse. We adapt an experimental Maze Search task previously used to study human planning, to show that in structured environments human planning is consistent with these two computational principles, in contrast to the state-of-the art model of depth-limited planning proposed in previous work. This result makes a *scientific contribution* by showing that human deviations from optimal policies are, at least in part, due to approximating planning by piecewise policies conditioned on structure for policy reuse. Our GenPlan framework makes an *engineering contribution* by showing how to actually build these principles into a working system. GenPlan is compute-efficient, because it achieves tractable inference over the underlying map structure by leveraging LLM-driven program generation (in contrast to enumerative search e.g. [Veness et al., 2011] ) and because it reduces the amount of planning compute through policy reuse.

We note that in our experiments planning varies between individuals, in line with variability observed in previous work Callaway et al. [2022]. Our model proposes a computational account explaining this variability as arising from how individuals may represent the same map in different ways. For example, depending on available cognitive resources, someone may form representations made up of coarser or finer patterns. In the limit, GenPlan can prioritize reconstruction accuracy and treat the entire environment as a single structural unit, solved by a globally optimal policy. Our implementation makes a simplifying assumption that that reconstruction and description weights are fixed and stable at population level, which works well to explain behavior in our experiment. Future work can further consider the stability and generalization of these parameters within and between individuals. General case solutions can be built to account for flexible cognitive resources, allowing the model to switch between map representations in response to changing cognitive demands. Future work can also examine how the weights should be chosen to optimally balance the computational costs of planning and memory, against utility.

**Limitations and future work.** Natural environment structure is often probabilistic, where the underlying building blocks of a given class differ superficially (e.g. square or rectangular city blocks; dunes of varied shapes and sizes). Future work can examine ways of capturing such representations,

as well as modeling how different goals shape cognitive map structure. For instance, people tend to perceive San Francisco as having a grid layout, even though its map reveals a complex structure that is merely grid-like. Such intuitions could arise from goal-dependent cognitive maps [Ho et al., 2022] – where a local grid model is actually good enough to plan a pedestrian shortcut across a neighborhood.

**Implications.** While planning cognition has been studied extensively, the domain of real-world planning remains underexplored. Reverse-engineering human planning can inform models that not only empower AI to better understand and assist humans, but also decrease environmental impact of AI algorithms, by enabling them to achieve effective policies with less compute. In contributing a proof of concept implementation, GenPlan brings new insights into human spatial planning, and takes a step toward building cost-efficient planning in AI.

## Acknowledgements

We are grateful to Dr. Ming Li (University of Waterloo) for funding Jeffrey Qin and Albert Yang's research assistanship, and providing Cole Wyeth with guidance and the freedom to pursue this cross-disciplinary project during PhD. Marta Kryven was supported by NSERC Discovery grant to Marta Kryven RGPIN-04045-25. We are grateful to Akshit Singh (Electrical Engineerin, IIT Jodhpur) for valuable discussion.

## References

Christian Bongiorno, Yulun Zhou, Marta Kryven, David Theurel, Alessandro Rizzo, Paolo Santi, Joshua Tenenbaum, and Carlo Ratti. Vector-based pedestrian navigation in cities, 2021.

Ugurcan Mugan, Seiichiro Amemiya, Paul S Regier, and A David Redish. Navigation through the complex world: The neurophysiology of decision-making processes. In *Habits: Their Definition, Neurobiology, and Role in Addiction*, pages 109–139. Springer, 2024.

Leslie Pack Kaelbling, Michael L Littman, and Anthony R Cassandra. Planning and acting in partially observable stochastic domains. *Artificial intelligence*, 101(1-2):99–134, 1998.

David Silver and Joel Veness. Monte-carlo planning in large pomdps. In *Advances in Neural Information Processing Systems, 2010*. Neural Information Processing Systems, 2010.

Aidan Curtis, Hao Tang, Thiago Veloso, Kevin Ellis, Joshua Tenenbaum, Tomás Lozano-Pérez, and Leslie Pack Kaelbling. Llm-guided probabilistic program induction for pomdp model estimation. *arXiv preprint arXiv:2505.02216*, 2025.

Marta Kryven, Suhyoun Yu, Max Kleiman-Weiner, Tomer Ullman, and Joshua Tenenbaum. Approximate planning in spatial search. *PLOS Computational Biology*, 20(11):e1012582, 2024.

Bas van Opheusden, Ionatan Kuperwajs, Gianni Galbiati, Zahy Bnaya, Yunqi Li, and Wei Ji Ma. Expertise increases planning depth in human gameplay. *Nature*, pages 1000–1005, 2023.

Ionatan Kuperwajs, Evan M Russek, Marcelo G Mattar, Wei Ji Ma, and Thomas L Griffiths. Looking deeper into the algorithms underlying human planning. *Trends in Cognitive Sciences*, 2025.

Stuart J Russell and Peter Norvig. *Artificial intelligence: a modern approach*. Pearson, 2016.

Yunzhe Liu, Marcelo G Mattar, Timothy EJ Behrens, Nathaniel D Daw, and Raymond J Dolan. Experience replay supports non-local learning. *BioRxiv*, pages 2020–10, 2020.

Hao Tang, Darren Key, and Kevin Ellis. Worldcoder, a model-based llm agent: Building world models by writing code and interacting with the environment. *arXiv preprint arXiv:2402.12275*, 2024.

Aidan Curtis, Tom Silver, Joshua B Tenenbaum, Tomás Lozano-Pérez, and Leslie Kaelbling. Discovering state and action abstractions for generalized task and motion planning. In *Proceedings of the AAAI conference on artificial intelligence*, volume 36, pages 5377–5384, 2022.

Satinder Singh, Michael James, and Matthew Rudary. Predictive state representations: A new theory for modeling dynamical systems. *arXiv preprint arXiv:1207.4167*, 2012.

Richard S Sutton, Doina Precup, and Satinder Singh. Between mdps and semi-mdps: A framework for temporal abstraction in reinforcement learning. *Artificial intelligence*, 112(1-2):181–211, 1999.

Jerry A Fodor. *The language of thought*, volume 5. Harvard university press, 1975.

Brenden M Lake and Steven T Piantadosi. People infer recursive visual concepts from just a few examples. *Computational Brain & Behavior*, 3(1):54–65, 2020.

Benjamin Pitt, Stephen Ferrigno, Jessica F Cantlon, Daniel Casasanto, Edward Gibson, and Steven T Piantadosi. Spatial concepts of number, size, and time in an indigenous culture. *Science Advances*, 7(33):eabg4141, 2021.

Lucas Tian, Kevin Ellis, Marta Kryven, and Josh Tenenbaum. Learning abstract structure for drawing by efficient motor program induction. *Advances in Neural Information Processing Systems*, 33, 2020.

Tessa Verhoef, Simon Kirby, and Bart De Boer. Emergence of combinatorial structure and economy through iterated learning with continuous acoustic signals. *Journal of Phonetics*, 43:57–68, 2014.

Martin Rohrmeier. Towards a formalization of musical rhythm. In *ISMIR*, pages 621–629, 2020.

Matthias Hofer, Tuan Anh Le, Roger Levy, and Josh Tenenbaum. Learning evolved combinatorial symbols with a neuro-symbolic generative model. *arXiv preprint arXiv:2104.08274*, 2021.

Sugandha Sharma, Aidan Curtis, Marta Kryven, Josh Tenenbaum, and Ila Fiete. Map induction: Compositional spatial submap learning for efficient exploration in novel environments. *International Conference of Learning Representations*, 2022.

William P McCarthy, Robert D Hawkins, Haoliang Wang, Cameron Holdaway, and Judith E Fan. Learning to communicate about shared procedural abstractions. *arXiv preprint arXiv:2107.00077*, 2021.

Iain G Johnston, Kamaludin Dingle, Sam F Greenbury, Chico Q Camargo, Jonathan PK Doye, Sebastian E Ahnert, and Ard A Louis. Symmetry and simplicity spontaneously emerge from the algorithmic nature of evolution. *Proceedings of the National Academy of Sciences*, 119(11): e2113883119, 2022.

Daniel D Dilks, Joshua B Julian, Jonas Kubilius, Elizabeth S Spelke, and Nancy Kanwisher. Mirror-image sensitivity and invariance in object and scene processing pathways. *Journal of Neuroscience*, 31(31):11305–11312, 2011.

Steven A Marchette, Lindsay K Vass, Jack Ryan, and Russell A Epstein. Anchoring the neural compass: coding of local spatial reference frames in human medial parietal lobe. *Nature neuroscience*, 17(11):1598, 2014.

Stephen M Kosslyn, Herbert L Pick Jr, and Griffin R Fariello. Cognitive maps in children and men. *Child development*, pages 707–716, 1974.

Albert Stevens and Patty Coupe. Distortions in judged spatial relations. *Cognitive psychology*, 10(4):422–437, 1978.

Stephen C Hirtle and John Jonides. Evidence of hierarchies in cognitive maps. *Memory & cognition*, 13(3):208–217, 1985.

Jeremy N Bailenson, Michael S Shum, and David H Uttal. The initial segment strategy: A heuristic for route selection. *Memory & Cognition*, 28(2):306–318, 2000.

Nora Newcombe, Janellen Huttenlocher, Elisabeth Sandberg, Eunhui Lie, and Sarah Johnson. What do misestimations and asymmetries in spatial judgement indicate about spatial representation? *Journal of Experimental Psychology: Learning, Memory, and Cognition*, 25(4):986, 1999.

Jan M Wiener and Hanspeter A Mallot. 'fine-to-coarse' route planning and navigation in regionalized environments. *Spatial cognition and computation*, 3(4):331–358, 2003.

Ranxiao Frances Wang and James R Brockmole. Human navigation in nested environments. *Journal of Experimental Psychology: Learning, Memory, and Cognition*, 29(3):398, 2003.

Jan Balaguer, Hugo Spiers, Demis Hassabis, and Christopher Summerfield. Neural mechanisms of hierarchical planning in a virtual subway network. *Neuron*, 90(4):893–903, 2016.

Momchil S Tomov, Samyukta Yagati, Agni Kumar, Wanqian Yang, and Samuel J Gershman. Discovery of hierarchical representations for efficient planning. *PLoS computational biology*, 16(4): e1007594, 2020.

Brenden M Lake, Ruslan Salakhutdinov, and Joshua B Tenenbaum. Human-level concept learning through probabilistic program induction. *Science*, 350(6266):1332–1338, 2015.

Joshua B Tenenbaum, Charles Kemp, Thomas L Griffiths, and Noah D Goodman. How to grow a mind: Statistics, structure, and abstraction. *science*, 331(6022):1279–1285, 2011.

Marta Kryven, Tomer D Ullman, William Cowan, and Joshua B Tenenbaum. Plans or outcomes: How do we attribute intelligence to others? *Cognitive Science*, 45(9):13–41, 2021.

Maya Geva-Sagiv, Soyeon Jun, Marta Kryven, Josh Tenenbaum, Erie D. Boorman, Randy O'Reilly, Jack J. Lin, Ignacio Saez, and Charan Ranganath. Fronto-hippocampal synchronization in rapid spatial learning in humans. *Current Biology*, 2025. Under review.

Omid Madani, Steve Hanks, and Anne Condon. On the undecidability of probabilistic planning and related stochastic optimization problems. *Artificial Intelligence*, 147(1-2):5–34, 2003.

Quentin JM Huys, Níall Lally, Paul Faulkner, Neir Eshel, Erich Seifritz, Samuel J Gershman, Peter Dayan, and Jonathan P Roiser. Interplay of approximate planning strategies. *Proceedings of the National Academy of Sciences*, 112(10):3098–3103, 2015.

Mark K Ho, David Abel, Carlos G Correa, Michael L Littman, Jonathan D Cohen, and Thomas L Griffiths. People construct simplified mental representations to plan. *Nature*, 606(7912):129–136, 2022.

J. Rissanen. Modeling by shortest data description. *Automatica*, 14(5):465–471, 1978. ISSN 0005-1098. doi: [https://doi.org/10.1016/0005-1098\(78\)90005-5](https://doi.org/10.1016/0005-1098(78)90005-5). URL <https://www.sciencedirect.com/science/article/pii/0005109878900055>.

Celeste Kidd, Steven T Piantadosi, and Richard N Aslin. The goldilocks effect: Human infants allocate attention to visual sequences that are neither too simple nor too complex. *PloS one*, 7(5):e36399, 2012.

Samuel J Cheyette and Steven T Piantadosi. A unified account of numerosity perception. *Nature human behaviour*, 4(12):1265–1272, 2020.

Mehdi Keramati, Peter Smittenaar, Raymond J Dolan, and Peter Dayan. Adaptive integration of habits into depth-limited planning defines a habitual-goal-directed spectrum. *Proceedings of the National Academy of Sciences*, 113(45):12868–12873, 2016.

Diogo R Ferreira. The impact of the search depth on chess playing strength. *ICGA journal*, 36(2):67–80, 2013.

Josef M Unterrainer, Benjamin Rahm, Christoph P Kaller, Rainer Leonhart, K Quiske, K Hoppe-Seyler, C Meier, C Müller, and Ulrike Halsband. Planning abilities and the tower of london: is this task measuring a discrete cognitive function? *Journal of clinical and experimental neuropsychology*, 26(6):846–856, 2004.

Frederick Callaway, Bas van Opheusden, Sayan Gul, Priyam Das, Paul M Krueger, Thomas L Griffiths, and Falk Lieder. Rational use of cognitive resources in human planning. *Nature Human Behaviour*, 6(8):1112–1125, 2022.

Carlos G Correa, Sophia Sanborn, Mark K Ho, Frederick Callaway, Nathaniel D Daw, and Thomas L Griffiths. Exploring the hierarchical structure of human plans via program generation. *Cognition*, 255:105990, 2025.

Aaron Wilson, Alan Fern, and Prasad Tadepalli. Transfer learning in sequential decision problems: A hierarchical bayesian approach. In *Proceedings of ICML Workshop on Unsupervised and Transfer Learning*, pages 217–227. JMLR Workshop and Conference Proceedings, 2012.

David Silver, Julian Schrittwieser, Karen Simonyan, Ioannis Antonoglou, Aja Huang, Arthur Guez, Thomas Hubert, Lucas Baker, Matthew Lai, Adrian Bolton, et al. Mastering the game of go without human knowledge. *nature*, 550(7676):354–359, 2017.

Sam Acquaviva, Yewen Pu, Marta Kryven, Theodoros Sechopoulos, Catherine Wong, Gabrielle Ecanow, Maxwell Nye, Michael Tessler, and Josh Tenenbaum. Communicating natural programs to humans and machines. *Advances in Neural Information Processing Systems*, 35:3731–3743, 2022.

Elizabeth S. Spelke and Katherine D. Kinzler. Core knowledge. *Developmental Science*, 10(1):89–96, 2007.

Stanislas Dehaene, Véronique Izard, Pierre Pica, and Elizabeth Spelke. Core knowledge of geometry in an amazonian indigene group. *Science*, 311(5759):381–384, 2006.

Sreejan Kumar, Carlos G Correa, Ishita Dasgupta, Raja Marjieh, Michael Hu, Robert D. Hawkins, Jonathan Cohen, Nathaniel Daw, Karthik R Narasimhan, and Thomas L. Griffiths. Using natural language and program abstractions to instill human inductive biases in machines. In Alice H. Oh, Alekh Agarwal, Danielle Belgrave, and Kyunghyun Cho, editors, *Advances in Neural Information Processing Systems*, 2022. URL <https://openreview.net/forum?id=buXZ7nIqiwE>.

Wen-Ding Li, Keya Hu, Carter Larsen, Yuqing Wu, Simon Alford, Caleb Woo, Spencer M Dunn, Hao Tang, Michelangelo Naim, Dat Nguyen, et al. Combining induction and transduction for abstract reasoning. *arXiv preprint arXiv:2411.02272*, 2024.

Marcel Binz, Elif Akata, Matthias Bethge, Franziska Brändle, Fred Callaway, Julian Coda-Forno, Peter Dayan, Can Demircan, Maria K. Eckstein, Noémi Éltető, Thomas L. Griffiths, Susanne Haridi, Akshay K. Jagadish, Li Ji-An, Alexander Kipnis, Sreejan Kumar, Tobias Ludwig, Marvin Mathony, Marcelo Mattar, Alireza Modirshanechi, Surabhi S. Nath, Joshua C. Peterson, Milena Rmus, Evan M. Russek, Tankred Saanum, Natalia Scharfenberg, Johannes A. Schubert, Luca M. Schulze Buschoff, Nishad Singhi, Xin Sui, Mirko Thalmann, Fabian Theis, Vuong Truong, Vishaal Udandarao, Konstantinos Voudouris, Robert Wilson, Kristin Witte, Shuchen Wu, Dirk Wulff, Huadong Xiong, and Eric Schulz. Centaur: a foundation model of human cognition, 2024. URL <https://arxiv.org/abs/2410.20268>.

Jacob Feldman. Tuning your priors to the world. *Topics in cognitive science*, 5(1):13–34, 2013.

Mark Towers, Ariel Kwiatkowski, Jordan Terry, John U Balis, Gianluca De Cola, Tristan Deleu, Manuel Goulão, Andreas Kallinteris, Markus Krimmel, Arjun KG, et al. Gymnasium: A standard interface for reinforcement learning environments. *arXiv preprint arXiv:2407.17032*, 2024.

Yaqi Xie, Chen Yu, Tongyao Zhu, Jinbin Bai, Ze Gong, and Harold Soh. Translating natural language to planning goals with large-language models. *arXiv preprint arXiv:2302.05128*, 2023.

Wasu Top Piriyakulkij, Yichao Liang, Hao Tang, Adrian Weller, Marta Kryven, and Kevin Ellis. Poe-world: Compositional world modeling with products of programmatic experts. *arXiv preprint arXiv:2505.10819*, 2025.

Joel Veness, Kee Siong Ng, Marcus Hutter, William Uther, and David Silver. A monte-carlo aixi approximation. *Journal of Artificial Intelligence Research*, 40:95–142, 2011.

## A Code availability

The Gen-POMCP implementation is available here: <https://anonymous.4open.science/r/GenPlan-FBCD/README.md>

## B Performance Bounds for Structure-Based Planning

In structured environments Gen-POMCP can explore the environment faster than Naive-POMCP (using fewer rollouts and in less time) by taking advantage of limited resources. However, it simplifies the planning problem by entirely exploring each fragment it enters before moving to the next. This heuristic can result in longer overall paths taken to search the environments. It is reasonable to ask by how much the global Naive-POMCP can actually improve on the path length taken by Gen-POMCP (and specifically the Structure-Based Planner).

Below give a sense of this answer by sketching a proof that considers the limit in which each planner fully optimizes its respective objective: Naive-POMCP follows the Bayes-optimal plan in each fragment and Gen-POMCP follows the Bayes-optimal global policy for the maze. We bound the cost difference according to expected and worst-case cost in steps (the latter is more analytically tractable).

**Expected and worst-case** The expected number of steps it takes for a policy to explore a maze is the average over the length of path this policy takes to reach uniformly sampled exit locations. The worst-case number of steps is the largest number of steps that the policy could take for some exit position. This is bounded below by the number of steps required to fully explore the maze.

**Lemma 1.** *There exists a fragment of size  $n \times n$  which takes  $O(n^2)$  steps to search in expectation, and to explore fully.*

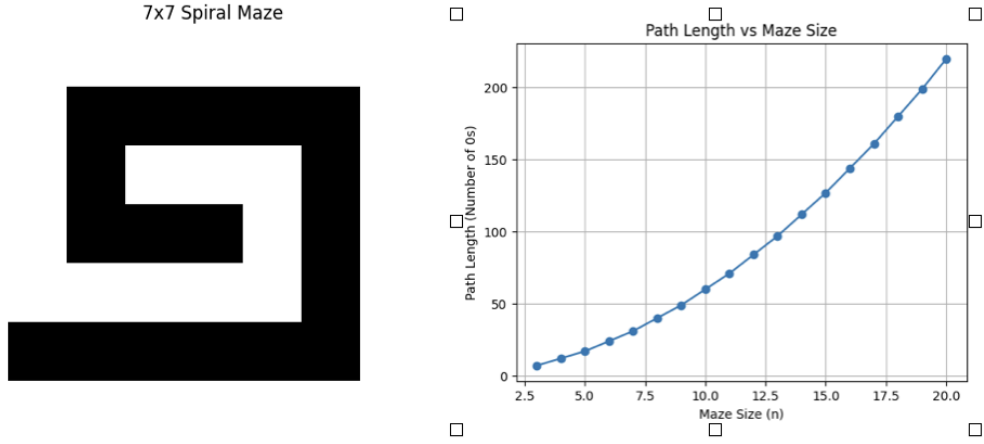


Figure 5: Consider a maze with a spiral wall - the white cells indicate traversable floor, and black indicate intraversable wall. Simulating these environments shows that the maximal length of path (white cells) in the environment grows as  $\approx \frac{1}{2}n^2$ .

*Proof.* Consider a fragment with the maximum spiral path (e.g. Figure 5). The length of this path scales quadratically with  $n$ . In particular, following a spiral path takes a series of four legs at each depth, and the length of every other leg reduces by two (one for the wall and one for the path itself).

This yields

$$\begin{aligned}
n + \sum_{i=0}^{\lfloor n/2 \rfloor - 1} 2(n-2i-1) &= \frac{n}{2}2n - 4\frac{(n/2)(n/2+1)}{2} + O(n) \\
&= \frac{1}{2}n^2 + O(n)
\end{aligned} \tag{3}$$

□

**Theorem 2.** *In the an  $n \times n$  maze, the expected number of steps taken by SBP may exceed the expected number of steps of an optimal policy by  $\Omega(n^2)$ .*

*Proof.* Build a fragment by adjoining an empty room and a spiral by a single door at a corner. Now connect the two fragments by adding a door between the empty rooms in the opposite corner. Assume the size of the empty rooms is such that the optimal algorithm can find the exit with probability  $1/2$  by checking each empty room, but the SBP algorithm must explore entirely the first fragment that it enters. With probability  $3/4$ , the exit is not in the first empty room, so it must explore the spiral, which takes time  $\Omega(n^2)$  to fully explore by Lemma 1. The spiral also must be exited, so around  $n^2$  steps are spent when the exit is in the other empty room (in this case the optimal planner finds immediately by checking each room). Since the optimal planner takes only a constant number of steps to check each empty room, and then behaves identically to the SBP, the expected cost when the exit is in any other location is asymptotically the same, so the expected cost difference is roughly  $\frac{1}{4}n^2 = \Omega(n^2)$ . □

**Theorem 3.** *The number of steps to fully explore a maze is  $O(n^2)$ .*

*Proof.* Consider a  $v$ -vertex connected graph. The maximum width (roughly achievable by the spiral) is  $v$ , leading to a naive bound of  $O(v^2) = O(n)$ . This can be improved to  $O(v)$  by running a depth-first search. Since there are 4 movement directions the degree of this graph is 4 meaning the maximum number of backtracks to a vertex is 3, which immediately gives  $4v$ . However, in a depth first search there is only one backtrack from each vertex is 1, which leads to an easy inductive proof that the bound is  $O(2v - 1)$  regardless of degree, yielding  $2n^2 - 1 = O(n^2)$ . Note that further improvements should be possible by considering the number of walls required to induce the worst-case topology. □

This implies that the Bayes-optimal policy has  $O(n^2)$  expected cost (since its *expected* cost must be at least as good as the *expected* cost of exhaustive search), regardless of the maze. Together, Lemma 1 and Theorem 3 demonstrate that the SBP heuristic does not damage the (asymptotic) expected cost in the worst maze.

**Theorem 4.** *Assume that an  $n \times n$  maze is fragmented in such a way that any time a fragment is entered, it can be fully explored before exiting, into  $c^2$  square  $(n/c) \times (n/2)$  fragments. The asymptotic expected cost is  $\Theta(n^2)$  in the worst such maze for the modular optimal and globally optimal policies.*

*Proof.* First, consider the global optimal policy. The additional requirements placed on the maze cannot make the  $O(n^2)$  bound in Theorem 3 worse, and we can get a matching lower bound by simply adjoining multiple spiral examples as in Lemma 1 and adding doors between them.

Now consider the modular optimal policy. It is clear that the globally optimal policy has an expected cost as least as low as the modular optimal policy (even in their respective worst mazes), by definition, so the  $\Omega(n^2)$  lower bound automatically carries over to the modular optimal policy. We assumed that the modular optimal policy takes the Bayes-optimal paths between fragments. This must be at least as good as the following strategy: mimic the global optimal policy, but any time a new fragment is entered, first explore it completely and return to the entrance. By Theorem 3, each such “extra” exploration detour takes at most  $2(\frac{n}{c})^2 - 1$  steps, and the return takes at most  $(\frac{n}{c})^2$  steps. The total is  $3(\frac{n}{c})^2 - 1$ . There are exactly  $c^2$  such detours, for  $4n^2 - c^2 = \Theta(n^2)$  extra steps. The global optimal policy also takes  $\Theta(n^2)$  steps. □

Therefore, in the worst case the modular algorithm is inferior by at least a constant factor of the total search time in expectation. Examining the proof of Theorem 4 yields a factor of 2.5 over our upper bound in Theorem 3, but presumably this can be improved substantially since a lot of exploration is being redone after the detours.

**Improving expected cost upper bounds** Substantial improvements to the worst-case cost bound in Theorem 3 are easy to obtain when the proof is applied to expected cost by e.g. noting that the depth-first search visits at least one new cell every two steps, meaning that there is clearly at least a  $1/4$  chance of finding the exit after  $n^2$  steps, or by noting that the true number of “vertices” is reduced by walls. These improvements seem to apply equally to the modular and global optimal policies, and probably do not affect our constants much.

For worst-case cost, the situation is similar. However, the worst-case cost analysis simplifies significantly with the additional assumption that transitions between fragments are negligible (say, if they all branch off from a central room). This observation is trivial but worth stating explicitly:

**Theorem 5.** *When the cost to transition between fragments is negligible, each has one entrance, and there is no line-of-sight across fragments, the modular algorithm has the same worst-case step count as the optimal algorithm.*

*Proof.* In the worst case, the optimal algorithm must explore each fragment, and since there is only one entrance to each fragment it is not possible to gain any advantage by exiting a fragment before it has been fully explored.  $\square$

## C Experimental Environments

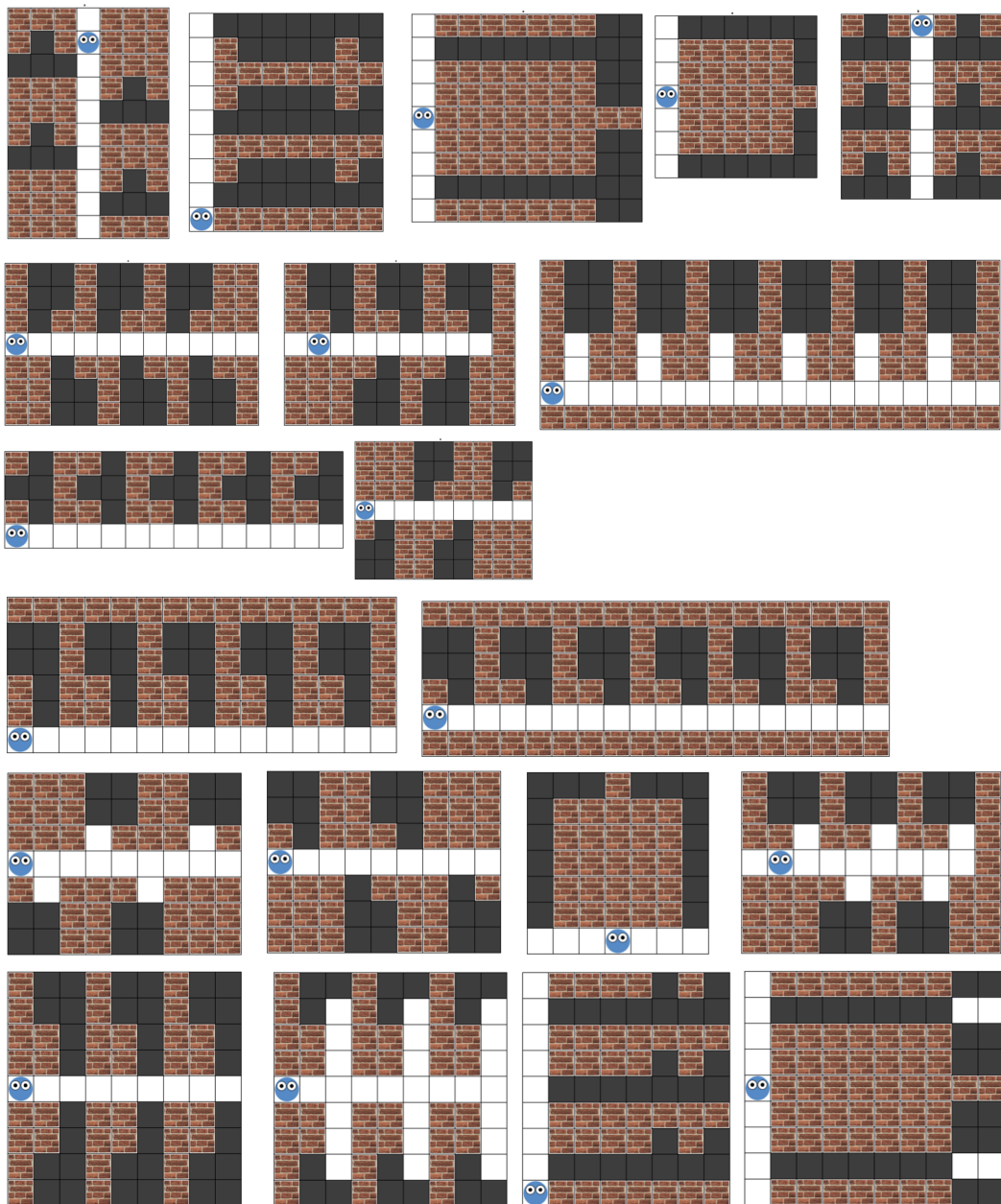


Figure 6: Environments used in Behavioral Experiment 1.

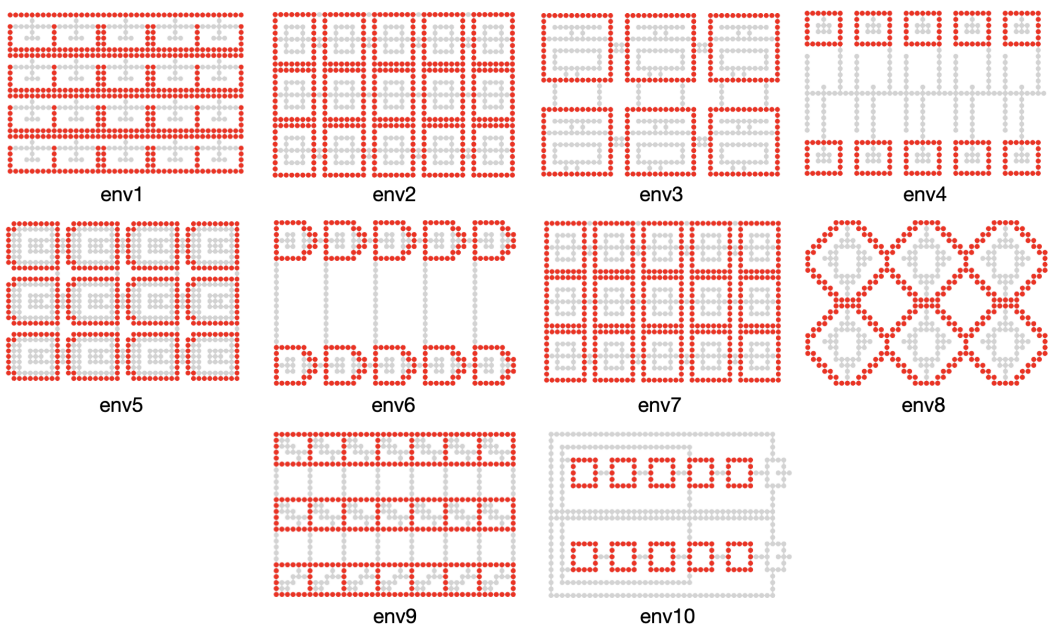


Figure 7: Environments used in Simulation Experiment 2.

## D Additional results - simulation experiment

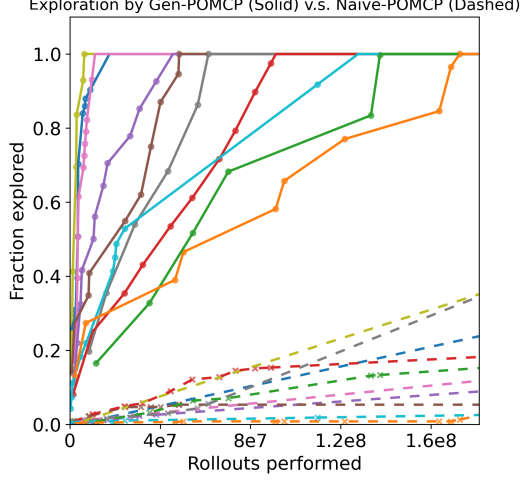


Figure 8: The fractions of each environment searched by Gen-POMCP and Naive-POMCP given identical computational budget. Gen-POMCP requires fewer rollouts and saves computing costs. Each environment is shown in a different color (see also Figure 4.)

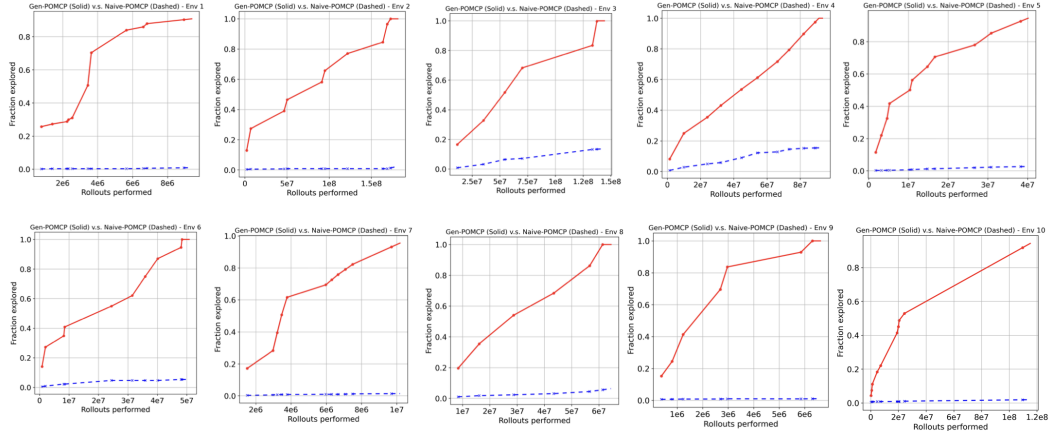


Figure 9: The fractions of each environment searched by Gen-POMCP and Naive-POMCP given identical computational budget. In each individual environment Gen-POMCP requires fewer rollouts and saves computing costs.)